

Received 24 August 2023, accepted 5 September 2023, date of publication 11 September 2023, date of current version 18 September 2023.

Digital Object Identifier 10.1109/ACCESS.2023.3313610

RESEARCH ARTICLE

DC Charger Circuit Optimization Design and Fast Charging and Discharging Mechanism Research

HAODONG SHEN¹, RONG YAN², JUNNAN ZHOU³, LIN PAN³, AND DONGJUNMING YANG^{ID}⁴

¹East China Electric Power Test Research Institute Company Ltd., Shanghai 200437, China

²Shanghai Aowei Technology Development Company Ltd., Shanghai 201203, China

³State Grid Shanghai Electric Municipality Power Company, Shanghai 200122, China

⁴Guizhou Power Grid Company Ltd., Guiyang 550002, China

Corresponding author: Junnan Zhou (53434641@qq.com)


This work was supported by the 2021 Shanghai “Science and Technology Innovation Action Plan” Technology Support Carbon Peak Carbon Neutralization Project “Research and Application of Intelligent Networked Charging Robot Based on Supercapacitor Energy Storage Technology” under Grant 21DZ1208500.

ABSTRACT With the advent of the era of new energy vehicles, the layout of charging piles is slightly lagging behind, and the charging efficiency of chargers is uneven, which leads to the problems of difficult charging and long charging time of electric vehicles. Therefore, market users put forward higher requirements for the charging efficiency of chargers. This paper first analyzes the circuit design principle and loss of the traditional charger, then designs a zero voltage switch(ZVS) half-bridge three-level DC/DC converter with high charging efficiency, and proposes a multi-stage constant current limiting charging strategy. Finally, through simulation and experimental verification, it is proved that the proposed strategy can strengthen the voltage regulation ability of the charger, and can achieve a stable current sharing state when charging.

INDEX TERMS Circuit design, charging strategy, DC/DC charger, working loss.

I. INTRODUCTION

With the continuous advancement of the new energy era, the number of electric vehicles has increased rapidly, and the problems of difficult charging and inconvenient charging of electric vehicles have become prominent. Due to the limited space and heat dissipation capacity in the vehicle, market users have put forward higher and higher requirements for the charging efficiency and power density of the charger [1]. As of the end of September 2022, the number of new energy vehicles in the country is 11.49 million. According to the data of the China Charging Alliance, as of June 2022, a total of 3.918 million charging infrastructures have been built nationwide. Under the background of the policy and the exponential growth trend of new energy vehicles, the national electric vehicle charging industry still has considerable market demand. The development demand of chargers is increasingly tending to high-energy rate density, low heating loss and convenient charging [2], [3], [4].

The associate editor coordinating the review of this manuscript and approving it for publication was Jiann-Jong Chen .

According to the installation location, the charger can be divided into on-board charger and off-board charger [5]. On-board charger installed in electric vehicles, generally through the household socket or AC charging pile for charging, charging voltage is usually 220 kV and single-phase AC. Because the volume and weight of the On-board charger should not be too large, and for single-phase power supply, all its output power is usually small, slow charging speed, gradually eliminated by the market [6]. At present, most electric vehicle chargers are non-vehicle chargers, whose input power is 380V three AC and output is DC. The volume of the off-board charger is not limited by space, and its power supply mode is three-phase current, so its charging speed is much faster than that of the vehicle charger, so it is widely used [7], [8], [9].

According to the different working frequency, the charger can be divided into power frequency charger and high frequency charger [10]. Power frequency charger operating frequency is low, resulting in filtering problems, so the volume of the filter is usually relatively large, so that the volume of the charger will increase accordingly [11]. Although the high frequency charger improves the efficiency

through the high frequency transformer, the increase of the switching frequency also brings the switching loss to rise linearly, so the soft switching technology is usually used to reduce its loss [12], [13].

According to the charging mode, electric vehicle charger can be divided into AC charger and DC charger [14]. The AC charger is limited because of its slow charging speed, while the DC charger has a fast charging speed and can provide sufficient power. The adjustment range of its output voltage and current is large, also known as 'fast charging' [15]. DC charger is generally divided into two stages, AC/DC converter and DC/DC converter. The DC/DC converter converts the high-voltage DC obtained by rectification into low-voltage DC for battery charging, and its comprehensive performance determines the operating efficiency of the charger [16], [17], [18].

The research focus of DC/DC converter technology gradually tends to be high frequency, multi-level and soft switching. In Reference [19], an online realtime optimization charging strategy for electric vehicle chargers is proposed for charging stations with renewable energy generation. This strategy can adjust the current charging power and the charging plan in the next 24 hours according to the real-time output of renewable energy and the real-time status information of electric vehicles. The charging optimization strategy can optimize the charging cost of the charging station to a certain extent and improve the load fluctuation when the charger is charging. In Reference [20], aiming at the problems of passive charging, high harmonics and low power factors of electric vehicle charging piles in the current market, the active power factor correction technology and double closed-loop direct voltage control strategy are used to design the three-phase half-bridge control circuit of the charger and its PI controller parameters. The control strategy can improve the charging power while ensuring that the charger has a stable output voltage. Reference [21] used soft switching technology to solve the problem of output voltage oscillation, and also reduced the conductor loss and improved the dynamic performance of the charger.

Based on the research of the above literature, this paper first analyzes the design principle and operating loss of the traditional charger, and on this basis, designs a ZVS half-bridge DC/DC converter topology and its control strategy. The simulation analysis proves that the proposed strategy can strengthen the voltage regulation ability of the charger and broaden the stability margin, and can stabilize the current sharing charging state.

II. DESIGN AND LOSS ANALYSIS OF FAST CHARGING OPTIMIZATION CIRCUIT FOR DC/DC CHARGER

A. TOPOLOGY OF ZVS HALF-BRIDGE THREE-LEVEL DC/DC CONVERTER

The initial development of electric vehicle charger is mainly composed of linear power supply. The charging efficiency is not high, and the volume is large and the capacity is small

[22]. Until the 1970s, with the invention of IGBT tubes that can withstand high voltage and high current, the development of charger power supply reached a new level. Switching power supply efficiency and power density are very high, very suitable for high power charger [23], [24], [25], [26]. Because of the urgent needs of the fast charging market, the charging power requirements of on-board chargers are increasing day by day, and modular design has become the mainstream development trend of chargers. At present, the dominant high-power DC/DC charger in the market is usually composed of a front-end AC/DC rectifier with power factor correction function and a rear-end DC/DC converter that controls the charging power [27], [28], [29], [30]. The structure is shown in Fig.1.

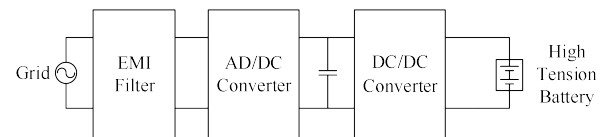


FIGURE 1. Power supply framework of vehicle charger.

The prestage rectifier corrects the power factor, and the post-stage DC/DC converter controls the charging power and voltage isolation. Therefore, the working efficiency of the post-stage DC/DC converter determines the overall performance of the DC/DC charger [31], [32], [33], [34], [35]. The DC/DC converter controlled by the traditional pulse width modulation method belongs to the hard switching type, that is, the voltage and current at both ends of the switch tube are not zero during the conduction and shutdown, and there is a cross between the two [36], [37], [38], [39]. The loss caused by the cross part is the switching loss. The switching process will produce a large peak voltage and switching noise, resulting in more serious electromagnetic interference problems [40], [41]. The switching process is shown in Fig.2.

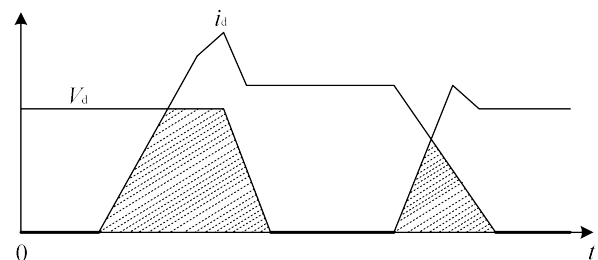


FIGURE 2. Hard switch working process.

Soft switch is by adding inductance and capacitance to the circuit, using resonance to change the period of voltage and current, which can eliminate the cross part of voltage and current in the process of hard switching, a good solution to the switching loss, noise interference and other issues [42], [43], the switching process is shown in Fig.3.

At present, there are two main types of soft-switching DC/DC converters on the market: zero-switching PWM and harmonic mode converter [44]. The single phase shift

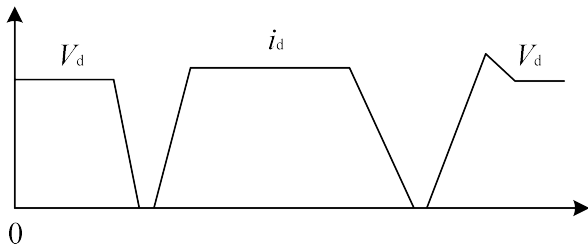


FIGURE 3. Soft switch working process.

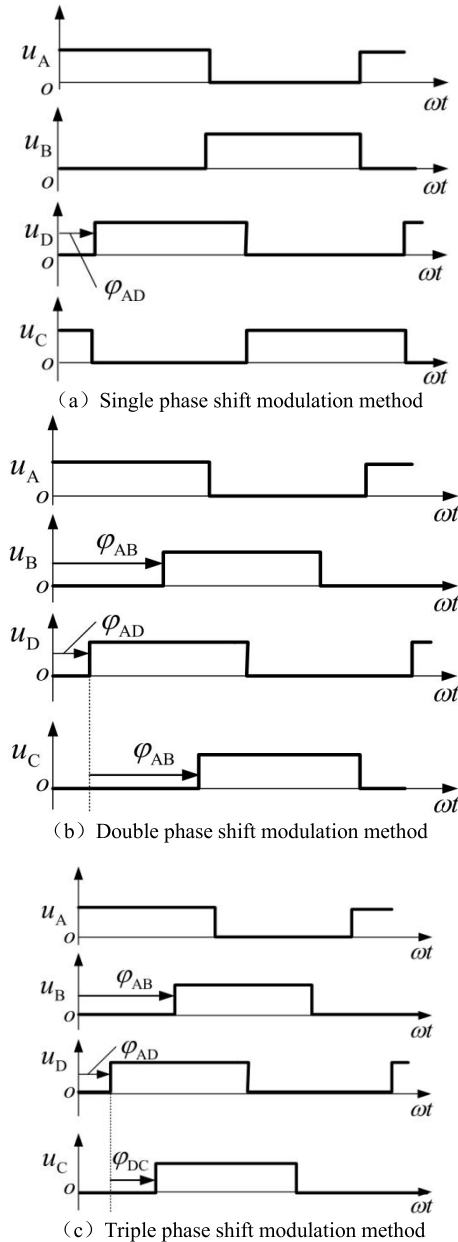


FIGURE 4. The basic phase shift modulation waveform of DC-DC converter.

modulation method is the earliest phase shift modulation method, which can realize the bidirectional transmission of energy, and its waveform is shown in Fig.4 (a). In order to

reduce the backflow power and weaken the current stress, a dual phase shift modulation method is proposed. The waveform is shown in Fig.4 (b). In order to expand the range of ZVS soft switching and improve the working efficiency, a triple phase shift modulation method is proposed. This modulation method can realize soft switching under no-load condition, reduce the peak value of current, improve the working efficiency and greatly reduce the volume of equipment. The waveform is shown in Fig.4 (c).

In this paper, a three-level DC/DC charger model based on ZVS half-bridge is designed and its loss is analyzed, which greatly improves the charging efficiency and power density of the charger. The topology is shown in Fig.5.

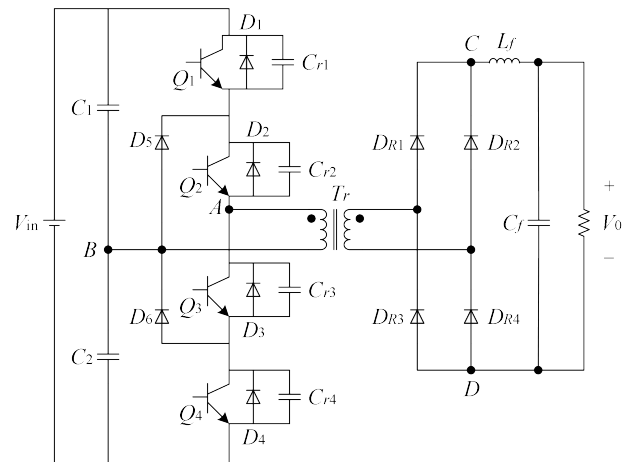


FIGURE 5. ZVS half-bridge three-level DC/DC converter topology.

In the Fig.5, V_{in} is the input voltage of the DC/DC converter. C_1 and C_2 are large-capacity input capacitors and their values are equal. Q_1 and Q_2 form the upper arm, and Q_3 and Q_4 form the lower arm. $D_1 \sim D_4$ are reverse parallel body diodes, which provide freewheeling paths for each mode. D_5 and D_6 are neutral point clamped diodes, whose role is to make the voltage clamp at the midpoint of the capacitor, so that the voltage of point A and point B has three states: $+V_{in}$, 0 and $-V_{in}$. T_r is the transformer of the converter, the role is mainly for electrical isolation and voltage conversion. The secondary full-bridge rectifier circuit of the converter is composed of $D_{R1} \sim D_{R4}$, which outputs DC pulse voltage to C and D points. $C_{r1} \sim C_{r4}$ are resonant capacitors and L_r is resonant inductor. C_f is the output filter capacitor and L_f is the output filter inductor. Their main functions are energy storage and filtering. C_f and L_f optimize the rectified DC pulse voltage to a DC voltage with small ripple, providing stable energy to the load. The relationship between the input voltage of the converter and its output voltage is:

$$V_o = \frac{DV_{in}}{2K} \tag{1}$$

D represents the duty cycle and has $D = 2T_{on}/T_s$, T_{on} represents the turn-on time, V_{in} represents the voltage between point A and point B, K is the ratio of transformer

turns. The output voltage can be controlled by changing the ratio of D to K , but the value of D cannot exceed 0.5.

B. PWM CONTROL OF ZVS HALF-BRIDGE THREE-LEVEL DC/DC CONVERTER

In the working process of the converter, by controlling the simultaneous conduction of Q_1 and Q_2 or Q_3 and Q_4 , the pulse voltage can be obtained at two points of A and B , and then the secondary pulse voltage of V_{in}/K can be obtained by the boosting effect of the transformer. Finally, through the rectification and filtering of the filter capacitor and inductance, the preset DC voltage is output. However, if $Q_1 \sim Q_4$ is turned on at the same time, the primary side will be short-circuited and the transformer will be burned out. Therefore, $Q_1 \sim Q_4$ cannot be turned on at the same time. In order to prevent magnetic core saturation, the conduction time of Q_1 and Q_2 is required to be consistent with the conduction time of Q_3 and Q_4 . The waveform at work is shown in Fig.6.

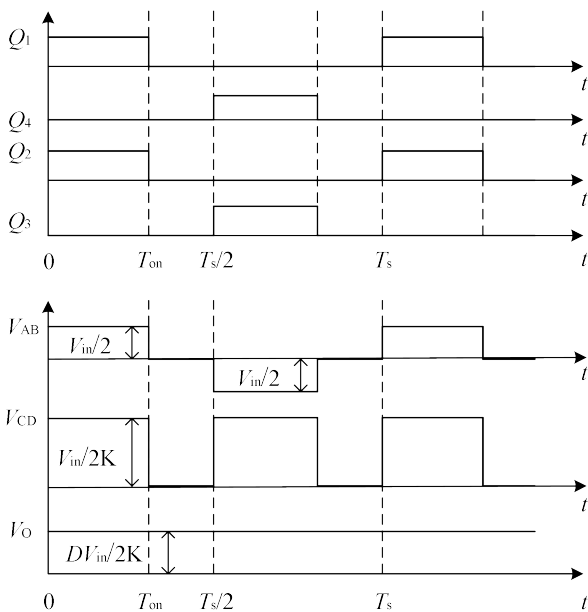


FIGURE 6. The basic PWM control method of the DC/DC converter.

In order to realize ZVS soft-switching control, it is needed to add control requirements to the above basic PWM control. At present, there are mainly four PWM control methods based on half-bridge three-level: one is to control Q_1 and Q_2 , Q_3 and Q_4 simultaneously on and off; the second is to fix the conduction time of Q_1 and Q_4 , and realize soft switching control by regulating the conduction time of Q_2 and Q_3 ; the third is to fix the conduction time of the switch tubes Q_2 and Q_3 , and realize the soft switching control by adjusting the conduction time of Q_1 and Q_4 . The fourth is to fix the conduction time of $Q_1 \sim Q_4$ as $T_s/2$, and control the conduction sequence of each switch tube by means of phase shift. The above four control methods are shown in Fig.7.

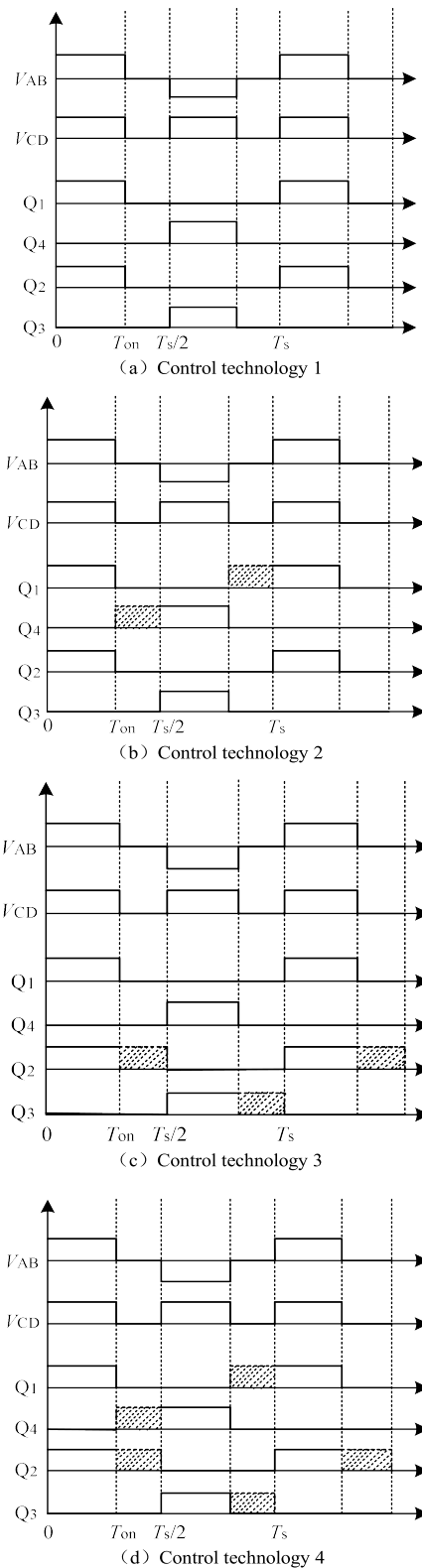


FIGURE 7. Four PWM control methods of the DC/DC converter.

By analyzing the four control methods described in Fig.7, it can be found that if the switch tubes of the upper arm are opened, the $V_{in}/2$ voltage can be obtained between A and B

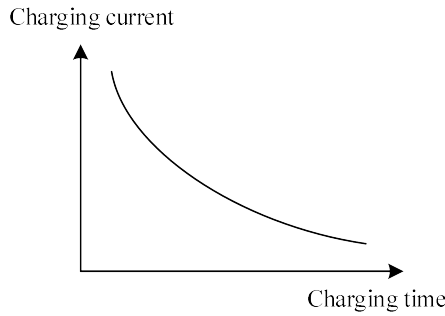


FIGURE 8. Mas charging curve.

points. Similarly, if the switch tubes of the lower bridge arm are opened, the $-V_{in}/2$ voltage can be obtained between *A* and *B* points. Therefore, as long as the conduction reclosing time of the bridge arm is consistent with the control method 1, any of the above four control methods can be used to control the output voltage, so the control methods 1 and 2 cannot achieve ZVS in the complete working process. Control methods 3 and 4 can achieve ZVS in a complete working cycle. However, it is difficult to achieve phase shift using the controller in real application scenarios. Therefore, control method 3 is used to achieve ZVS in engineering practice.

C. LOSS ANALYSIS OF ZVS HALF-BRIDGE THREE-LEVEL CONVERTER

With the continuous improvement of the power density requirements of the DC/DC charger, the switching frequency of the converter also needs to be increased to meet the requirements, but this will also increase the switching loss. Therefore, it is difficult for high-power converters to achieve high efficiency under hard switching conditions [45]. When the converter realizes ZVS, the cross part of voltage and current in the hard switching process can be eliminated, which solves the problem of switching loss. The losses of ZVS half-bridge three-level converter are mainly conduction loss and transformer loss [46].

1) CONDUCTION LOSS ANALYSIS

The conduction loss is the loss generated by the current flow when the converter is working. The calculation method is the square value of the conduction resistance R_{on} multiplied by the conduction current I_p . The expression is as follows:

$$\begin{aligned}
 P_{con} &= I_p^2 R_{on} \\
 &= \frac{1}{T} \left[\int_0^{t_0} 2I_1^2 R_{on} dt + \int_{t_0}^{t_2} I_1^2 R_{on} dt + \int_{t_3}^{t_4} 2I_{t34}^2 R_{on} dt \right. \\
 &\quad \left. + \int_{t_4}^{t_5} 2I_{t45}^2 R_{on} dt + \int_{t_5}^{t_6} 2I_{t56}^2 R_{on} dt \right] \quad (2)
 \end{aligned}$$

In the above equation, I_1 denotes the primary current of $t_0 \sim t_2$; I_{t34}^2 represents the primary current of $t_3 \sim t_4$; I_{t45}^2 represents the primary current of $t_4 \sim t_5$; I_{t56}^2 represents the primary current of $t_5 \sim t_6$; R_{on} represents the on-resistance.

Of which:

$$I_1 = I_p(t_0) \quad (3)$$

$$I_p = I_L(t)/K \quad (4)$$

$$I_p = I_2 \cos \omega_r(t - t_2) \quad (5)$$

$$I_{34} = I_p(t) = I_p(t_4) - \frac{V_{in}}{2L_r}(t - t_4) \quad (6)$$

$$I_{45} = I_p = -\frac{V_{in}}{2L_r}(t - t_4) \quad (7)$$

$$I_{56} = I_p(t) = -\frac{V_{in} - KV_o}{L_r + K^2L_f}(t - t_5) \quad (8)$$

2) TRANSFORMER LOSS ANALYSIS

Under the premise of keeping the capacity unchanged, increasing the operating frequency of the transformer can reduce its volume. Therefore, DC/DC charger usually adopts DC/DC high-frequency transformer, and its losses are mainly core loss and winding loss [47].

The core loss of high frequency transformer can be calculated by loss separation method. The method is as follows:

$$P_C = P_h + P_e + P_r = K_h f B^\beta + K_e f^2 B^2 + K_f f^{1.5} B^{1.5} \quad (9)$$

In the (9), K_r , K_e and K_h are residual loss coefficient, eddy current loss coefficient and hysteresis loss coefficient respectively. B represents the magnetic flux density; β denotes the magnetic material constant.

The loss generated by the current through the high-frequency transformer coil is called winding loss. DC/DC converters usually work in high frequency conditions, so the current flowing through the coil winding of high frequency transformer will produce skin effect and proximity effect. This situation will cause the utilization area of the winding resistance section to be smaller than its actual area, thereby increasing the winding loss. The winding loss can be calculated by Fourier decomposition of the winding current: the effective value of each harmonic current component can be obtained by Fourier decomposition, and then the AC resistance value under each harmonic is calculated, and the winding loss is obtained. The equation is as follows:

$$P_{rz} = R_{dc}(I_{dc}^2 + \sum_{n=1}^{\infty} I_n^2 F_{Rn}) \quad (10)$$

In the above equation, R_{dc} is the DC resistance of the winding coil; I_n is the n th harmonic current; F_{Rn} is the ratio of AC resistance to DC resistance under n th harmonic excitation.

III. RESEARCH ON CHARGING CONTROL STRATEGY OF DC/DC CHARGER

In the early stage of electric vehicle charger, the charging control strategy of voltage single closed-loop control was adopted. This strategy is simple and has good stability. However, this control strategy does not collect the output current of the charger, resulting in a lag in the response

of the charger to the sudden change of the load current. The emergence of the double closed-loop control strategy solves the above problems well. It uses the current inner loop and the voltage outer loop for double closed-loop cascade control, which can not only stably control the output voltage, but also quickly respond to the load current change, and realize the constant voltage current limiting charging. Based on the above charging strategy, this chapter proposes a control strategy based on modulation wave selection with better voltage regulation ability and margin.

A. CHARGER CHARGING METHOD

The Mas charging curve is recognized as the best charging curve for the electric vehicle charger to charge the power battery pack in the world. At present, most of the charging control methods and strategies are as close as possible to the Mas charging curve to reduce the phenomenon of gas evolution and prolong the charging and dis-charging times and service life of the battery. The Mas charging curve is shown in Fig.8.

There are many main charging methods for power batteries. At present, the commonly used charging methods are constant voltage, constant current, constant voltage current limiting and constant current voltage limiting. The charging voltage of the charger directly affects the charging efficiency. The common methods to improve the charging efficiency generally include increasing the operating frequency of the transformer and the parallel charger module. The latter usually produces the phenomenon of current imbalance during operation. Taking the parallel connection of two charger modules as an example, the control target of the parallel system is the given current value, and the control output is the charging voltage. In the actual working conditions, the output voltage of different modules is not completely consistent, so that the charging current is not balanced. Fig.9 is its equivalent circuit diagram.

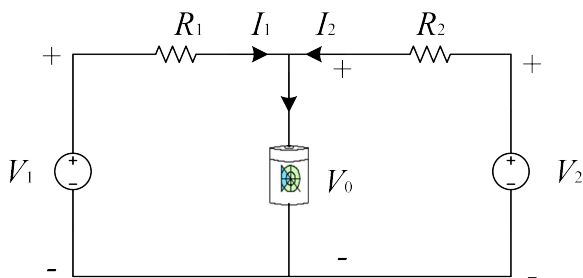


FIGURE 9. Parallel equivalent circuit of two charger modules.

In the Fig.9, V_0 is the load side voltage, V_1 and V_2 are the output voltages of the two modules respectively, and R_1 and R_2 are the output impedance. The output characteristics of the two modules are as follows:

$$V_1 = V_0 + I_1 R_1 \tag{11}$$

$$V_2 = V_0 + I_2 R_2 \tag{12}$$

It can be seen from the above equation that the equivalent internal resistance of the two charger modules from the parallel point to the sampling point is not completely consistent and the actual output voltage of the sampling point is inconsistent, which are the two main reasons for the unbalanced output current of the charger parallel module.

Taking the parallel connection of two charger modules as an example, n groups of control outputs are randomly generated for charge and discharge cycle experiments. The charging adopts constant current and constant voltage mode, the discharge adopts constant current mode, the inconsistency degree of equivalent internal resistance is expressed by x , the inconsistency degree of actual output voltage of sampling point is expressed by y , the current balance degree is expressed by z , the number of cycles is set to 500, and the steps are shown in Fig.10.

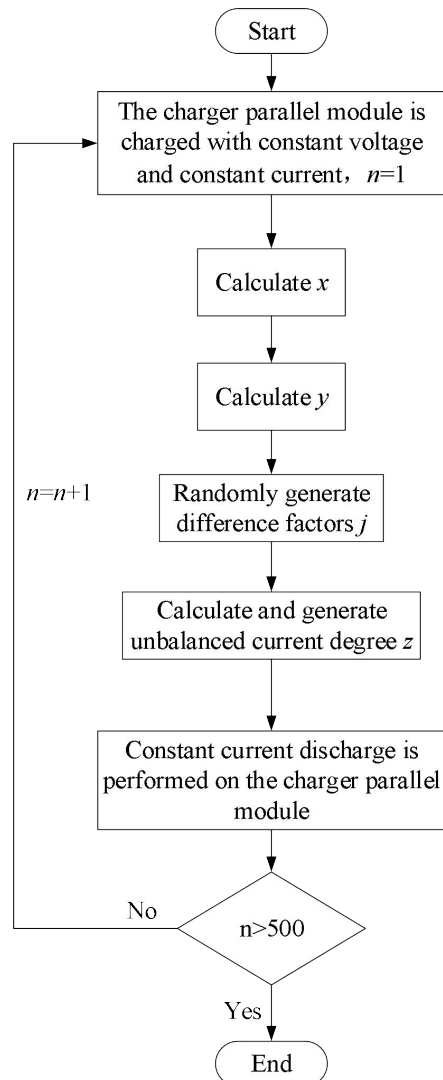


FIGURE 10. Parallel inconsistency analysis process of two charger modules.

After the above steps of simulation, you can get the results shown in Fig.11.

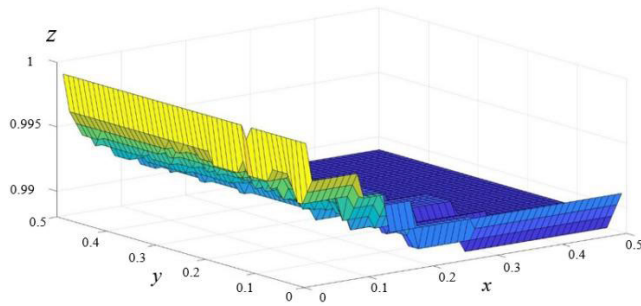


FIGURE 11. The influence of the inconsistency between the equivalent internal resistance and the actual output voltage on the current balance degree.

It can be found from Fig.11 that as the inconsistency between the actual output voltage and the equivalent internal resistance of the sampling point decreases, the current balance degree shows a nonlinear multivariate increase. Since the equivalent resistance between the load and the output module is generally small, the output voltage of the two modules is slightly different. It will immediately cause a large imbalance in the output current, and the output impedance difference between the two modules will amplify the imbalance, resulting in a very difficult balance control of the charger, and the control cost will also rise linearly. Therefore, this paper studies the charging process of the charger by increasing the operating frequency of the transformer.

B. CONSTANT VOLTAGE CURRENT LIMITING CHARGING CONTROL STRATEGY BASED ON DOUBLE CLOSED LOOP CASCADE CONTROL

The double closed-loop cascade control strategy is to embed the current inner loop control into the original voltage single closed-loop control, which can strengthen the response sensitivity of the control system to current changes. This strategy basically eliminates the shortcomings of poor anti-power supply and load disturbance ability of voltage single closed-loop control, and optimizes the dynamic adjustment ability of charger charging control system. The principle flow is shown in Fig.12.

The principle is to use the voltage outer loop to stabilize the output voltage u_o of the charger at a given voltage value U_{ref} , and the quasi-current reference value i'_{ref} of the current inner loop controller is taken from the output of the voltage outer loop controller. The value i'_{ref} is compared with the current limiting value I_{lim} , and the smaller value is selected as the actual current reference value i_{ref} of the current inner loop controller. The output current i_o of the charger does not exceed the charging current limiting I_{lim} in the current inner loop control mode, and the constant voltage current limiting charging is realized. The principle flow is shown in Fig.13.

In the Fig. 13, U_{ref} and I_{lim} are the voltage value and current limiting value of constant voltage charging respectively. u_o and i_o are the output voltage and current respectively. u_{err} and i_{err} are voltage and current error signals, respectively. $G_{cv}(s)$

and $G_{ci}(s)$ are voltage and current controllers, respectively. i'_{ref} and i_{ref} are the quasi-current reference value and the actual current reference value, respectively. u_r is the output modulation signal of the controller.

In the actual working condition of the battery, the internal resistance is small in the initial stage of charging. At this time, the voltage outer loop controller does not play a control role because its output quasi-current reference value is greater than the charging current limiting value I_{lim} . The entire double closed-loop cascade control system is equivalent to the current single loop control, which will make the charger work in a current limiting charging state. The internal resistance of the battery will increase with the increase of the remaining capacity, and the charging voltage will also increase, and reach the given value U_{ref} at a certain moment. At this time, the charging current limiting value will be greater than the quasi-current given value output by the voltage outer loop controller. The voltage outer loop controller begins to act on the actual control, so that the charger works in the constant voltage current limiting charging state. In the constant voltage limited current charging state, the charging current will gradually decrease with the increase of the equivalent internal resistance of the battery, until its value is equal to the battery trickle cut-off current, the charger ends the charging state.

The double closed-loop cascade control strategy can enhance the response sensitivity of the charger control system to current changes, and has a relatively stable control performance. However, from another perspective, it reduces the response sensitivity of the charger control system to current changes, reduces the stability margin, and increases the difficulty of control. However, the defect is not obvious when the charger is operated in a single module. When multiple charger modules are operated in parallel, these defects will be very significant, so the strategy is mostly used in the single-module control system of the charger in practical applications.

C. FORMATTING OF MATHEMATICAL COMPONENTS

Aiming at the problems of low voltage change sensitivity, small stability margin and high control difficulty of traditional double closed-loop cascade control strategy, a constant voltage and current limiting charging control strategy based on modulation wave selection control is proposed. This strategy can not only retain the advantages of high sensitivity and good dynamic performance of double closed-loop cascade control strategy to current change response, but also solve the defects of double closed-loop cascade control strategy. The principle of this control strategy is to split the voltage loop and current loop, and adjust their respective controllers separately, so that two modulation waves can be obtained. Finally, one of the above two modulation waves is selected as the actual modulation signal by adopting the set switching mode. This strategy adopts the switching method of small comparison, that is, comparing the amplitude of the two modulation waves, and then selecting the modulation

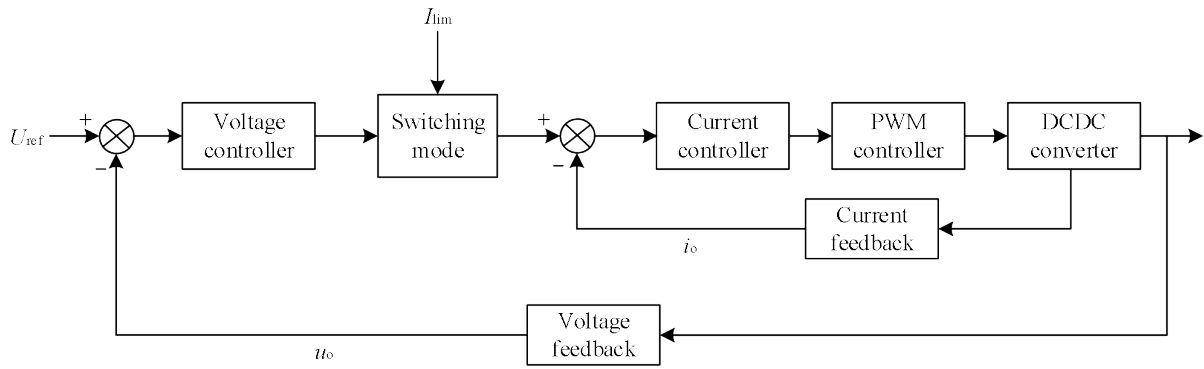


FIGURE 12. Double closed-loop cascade control strategy structure.

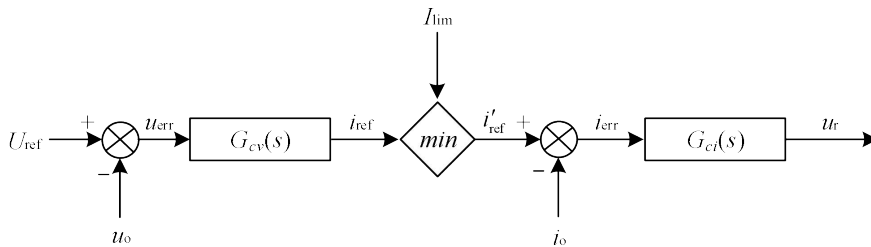


FIGURE 13. Principle Diagram of Double Closed Loop Cascade Control Strategy.

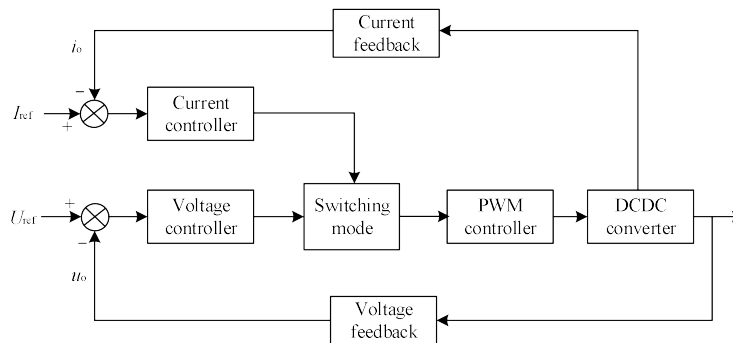


FIGURE 14. Modulation wave selection control system block diagram.

wave with small amplitude as the final modulation signal. Its control system structure is shown in Fig.14:

The principle of modulation wave selection control strategy is to select the modulation wave with small amplitude as the actual modulation signal by comparing the voltage modulation wave u_{r1} output by the voltage loop controller and the current modulation wave u_{r2} output by the current loop controller. With this switching method, the charger is capable of charging at both a constant voltage of U_{ref} and a constant current of I_{lim} . Because the logic control rule of taking small as the switching mode is equivalent to the intersection in the fuzzy control theory, the charger will not exceed the given value of the charging voltage and current in the whole charging process. The principle flow is shown in Fig.15.

In Fig.15, min represents the switching mode with small comparison, which is the core part of modulation wave

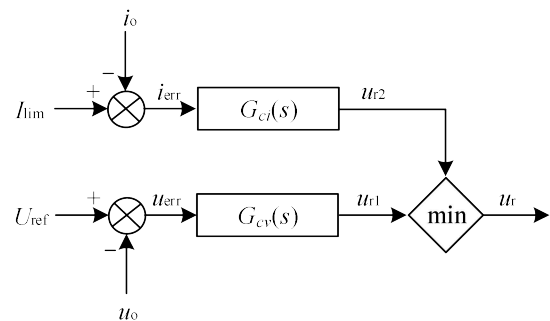


FIGURE 15. Modulation wave selection control strategy principle flow chart.

selection control. It adjusts the charging mode of the charger by continuously voltage modulation wave u_{r1} and current modulation wave u_{r2} output by current loop controller, and

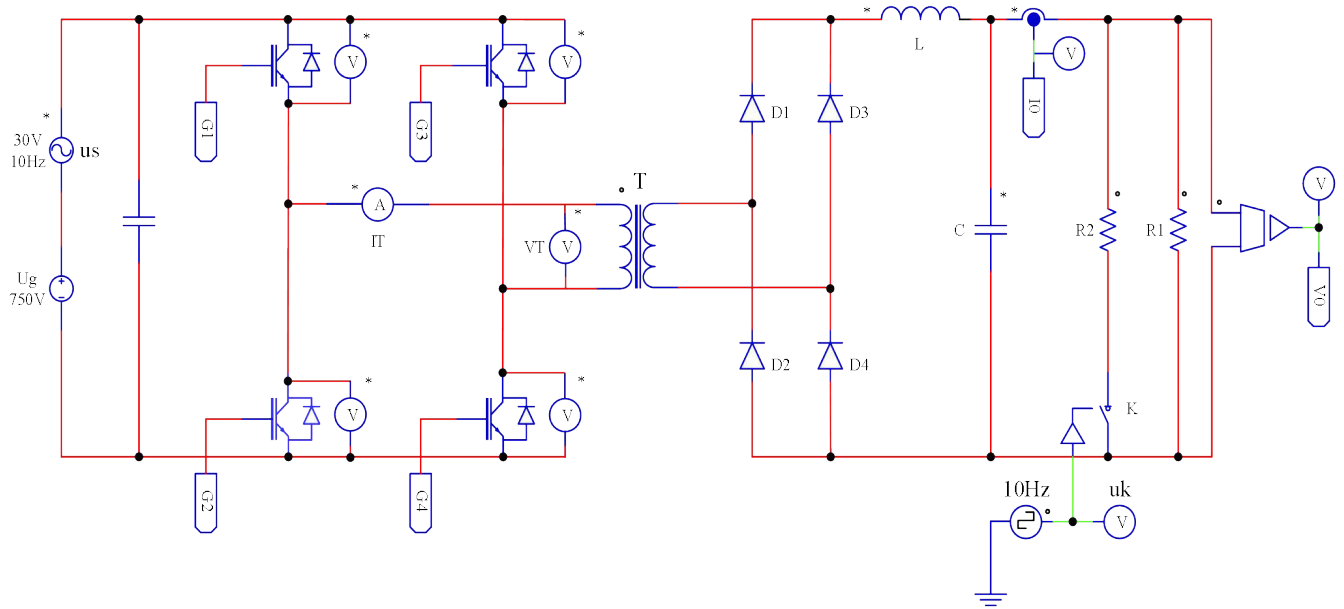


FIGURE 16. Simulation model of DC/DC converter.

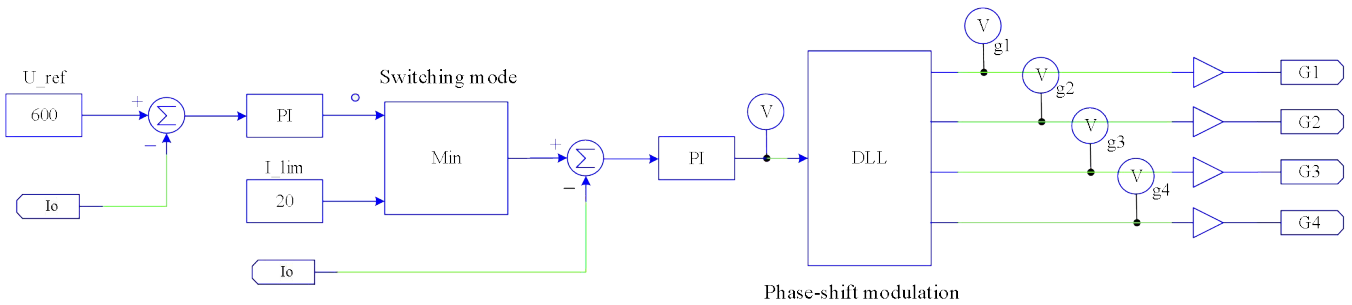


FIGURE 17. Double closed-loop control circuit.

selects the modulation wave with small amplitude as the actual modulation signal. The meanings of other parameters are consistent with the previous section.

In the actual working condition of the battery, the equivalent internal resistance is small at the beginning of charging, which will make the charging current i_o relatively large, resulting in the amplitude of the output modulation wave u_{r1} of the voltage loop controller is greater than the amplitude of the output modulation wave u_{r2} of the current loop controller. At this time, the charger works in the current single closed-loop control state, that is, charging with the current limit value I_{lim} constant current, and the charging voltage u_o also begins to gradually increase. When u_o rises to the voltage given value U_{ref} , u_{r2} begins to be greater than u_{r1} . At this time, the charger works in a voltage single closed-loop control state, that is, charging at a constant voltage U_{ref} , and the charging current will continue to decline until the charging is completed.

Comparing the two control strategies, it can be found that their common point is that when the charger works

in the current-limiting charging condition, it is a current single closed-loop control. In the constant voltage charging condition, the double closed-loop cascade control strategy is voltage single closed-loop control, and the modulation wave selection control strategy is double closed-loop control. Modulation wave selection control strategy not only retains the characteristics of high response sensitivity of double closed-loop cascade control strategy to current change, but also improves the sensitivity of charger control system to voltage change, which is very suitable for charger multi-module parallel control system.

In summary, the advantages and disadvantages of the common charging control strategies of electric vehicle chargers in recent years can be compared and summarized as shown in Table 1:

IV. SIMULATION VERIFICATION

In order to analyze the feasibility and superiority of the modulation wave selection control strategy proposed in this paper, the simulation model of the charger DC/DC

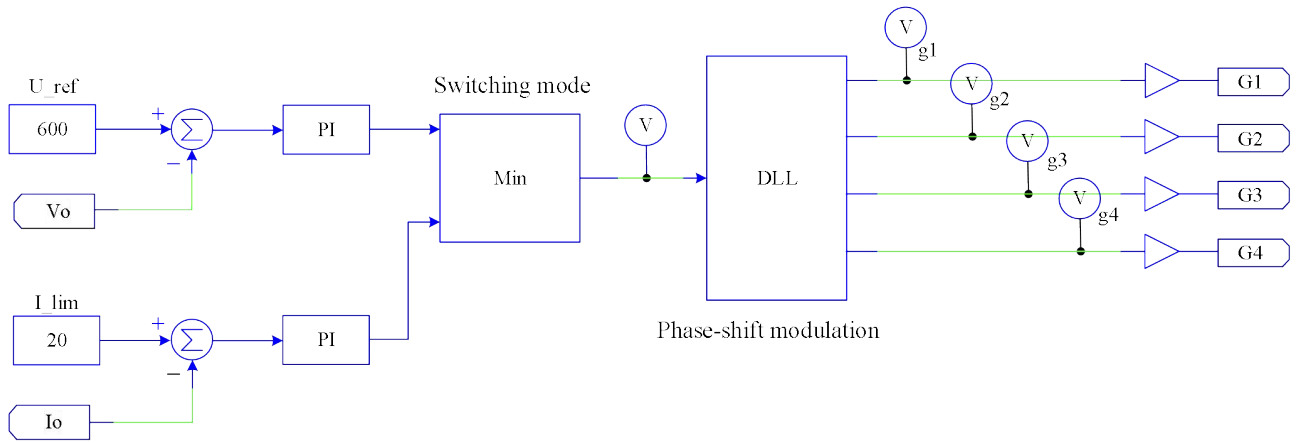


FIGURE 18. Modulation wave selection control circuit.

TABLE 1. Performance comparison table of charging control strategies in recent years.

Charging Control Strategy Name	Merit	Demerit
Voltage single closed-loop control strategy	The control circuit is simple and the stability is good.	The charger's response to the sudden change of load current lags behind.
Constant voltage current limiting charging control strategy based on double closed loop cascade control	It has high response sensitivity to current change and strong ability to resist power supply and load disturbance.	The small stability margin leads to the increase of control difficulty.
Constant voltage current limiting charging control strategy based on modulation wave selection control	It has high sensitivity to current and current change, large stability margin and good dynamic performance.	The stability will be reduced in the single module control system.

converter is built in this section. The constant voltage current limiting charging control strategy based on double closed-loop cascade control is set as the control group. The superiority of the proposed strategy is analyzed from two different perspectives of steady state and dynamic state.

A. BUILD SIMULATION MODEL

Fig. 16 is the charger DC/DC converter simulation model built in PSIM, where U_g represents the DC voltage input and U_s represents the AC power supply with a frequency of 100 Hz and an amplitude of 20 V, which is used to simulate the input voltage fluctuation. The 10 Hz pulse wave is used as the control signal of the switch K to simulate the removal and input of the load R_2 .

Fig. 17 shows the double closed-loop cascade control circuit, Fig. 18 is the modulation wave selection control circuit. Among them, the Min module represents a small function, the role is to switch between constant voltage and

current limiting charging mode. The DLL file is a phase shift modulation strategy.

B. ANALYSIS OF SIMULATION RESULTS

In order to compare the characteristics of the two proposed charging control strategies more comprehensively, this paper mainly simulates from three aspects: steady state and dynamic state, anti-load disturbance ability and anti-DC voltage disturbance ability, and compares and analyzes the simulation waveforms.

1) STEADY AND DYNAMIC SIMULATION

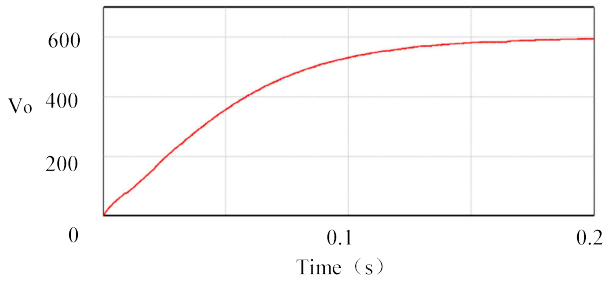
The purpose of steady-state and dynamic simulation experiments is to compare the dynamic adjustment sensitivity and steady-state performance of DC/DC converters under two different control strategies. The parameters of the simulation experiment are set as follows: the input DC voltage and output voltage are 750 V and 600 V respectively, the current limit is 25 A, and the load is 30 Ω . Fig. 15 is the output voltage waveform under the double closed-loop cascade control strategy, and Fig. 16 is the output voltage waveform under the modulation wave selection control strategy.

According to the Fig. 19, it takes 0.17 s for the charger to start to voltage stability, and the voltage ripple is 0.04%.

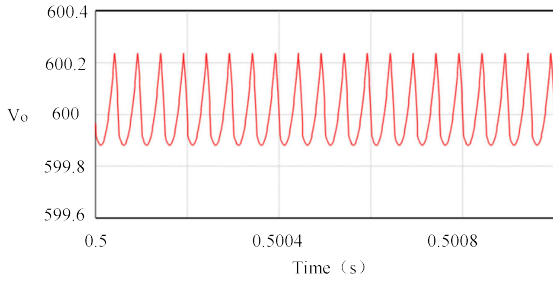
According to the Fig. 20, the output voltage stability time of the charger under the modulation wave selection control strategy is 0.03 s, and the voltage ripple is 0.02%. By comparing the output voltage waveforms of the charger under the two control strategies, it can be found that the output voltage ripple under the two control strategies is not much different, but the modulation wave selection control strategy has higher response sensitivity to the voltage, shorter adjustment time, and better dynamic performance than the double closed-loop cascade control strategy.

2) LOAD DISTURBANCE SIMULATION

The purpose of the load disturbance is to compare the anti-load disturbance ability under two different control strategies. The input and removal of the simulated load R_2 are controlled

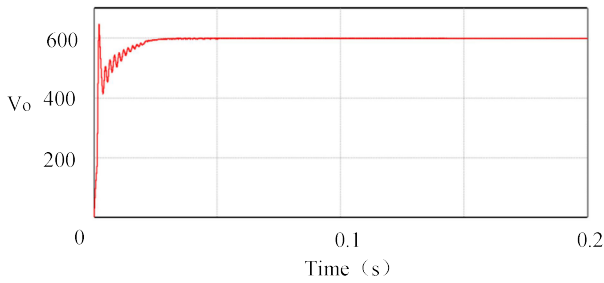


(a) Dynamic

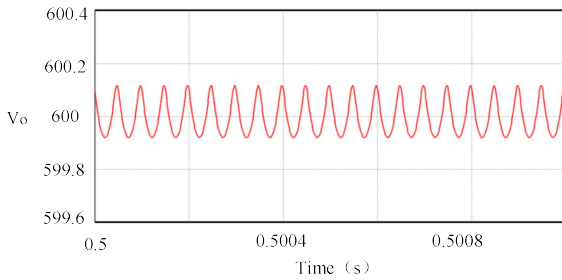


(b) Steady-state

FIGURE 19. Double closed-loop control strategy simulation waveform.



(a) Dynamic



(b) Steady-state

FIGURE 20. Modulation wave selection control strategy simulation waveform.

by the pulse signal u_k . The input is set to 750 V DC voltage, the output is set to 600 V voltage reference value, and the current limit value is set to 25 A. In order to simulate the switching of the load current between 10 A and 20 A, the resistance values of R_1 and R_2 are set to 60 Ω . Fig.21 is the output simulation waveform of the load disturbance of the charger under the double closed-loop cascade control strategy. Fig.22 is the output simulation waveform of the load disturbance of the charger under the modulation wave selection control strategy.

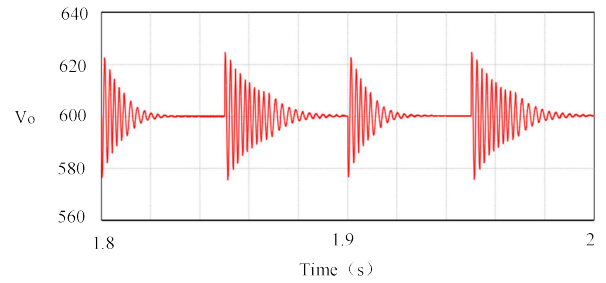


FIGURE 21. Double closed-loop cascade control strategy simulation waveform.

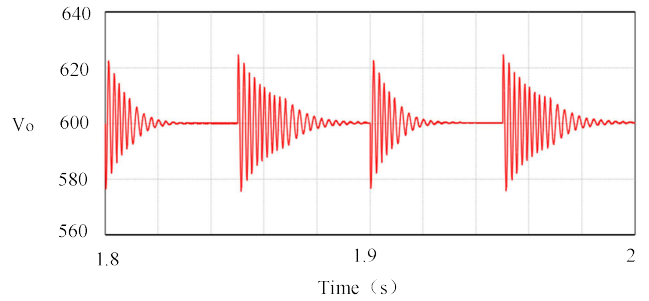


FIGURE 22. Modulation wave selection control strategy simulation waveform.

From the simulation waveforms of Fig.21 and Fig.22, it can be known that under the same load disturbance, the adjustment time of the charger converter to suppress the voltage fluctuation under the two control strategies is not much different, but the output voltage fluctuation amplitude using the modulation wave selection control strategy is much smaller than the output voltage fluctuation amplitude using the double closed-loop cascade control strategy.

3) POWER DISTURBANCE SIMULATION

The purpose of the simulation experiment of power disturbance is to compare the ability to resist power disturbance under two different control strategies. The output parameters are: DC voltage 750 V and superimposed with a disturbance AC voltage with a peak value of 30 V and a frequency of 10 Hz. The output voltage is set to 600 V, the current limit is set to 25 A, and the load is set to 30 Ω . The simulation results are shown in Fig.23 and Fig.24.

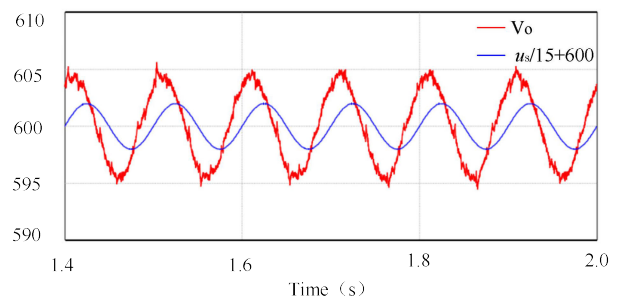


FIGURE 23. Double closed-loop control strategy disturbance simulation.

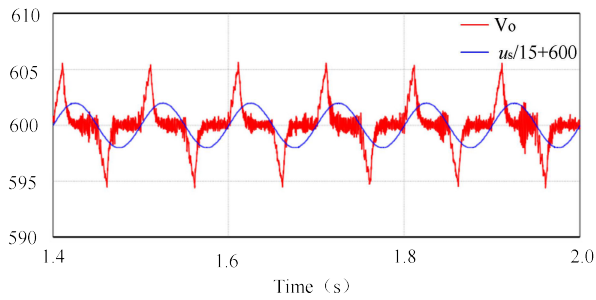


FIGURE 24. Modulation wave selection control strategy simulation.

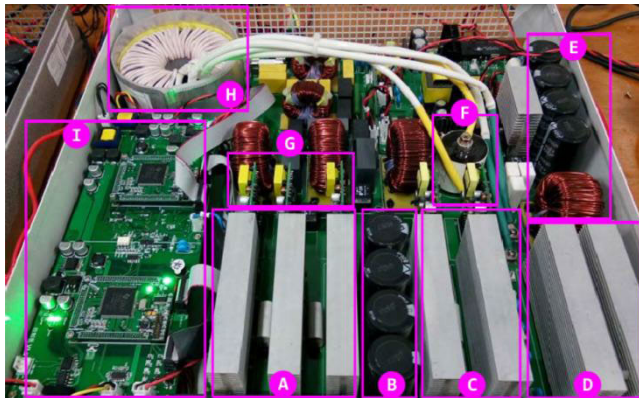


FIGURE 25. Prototype module platform.

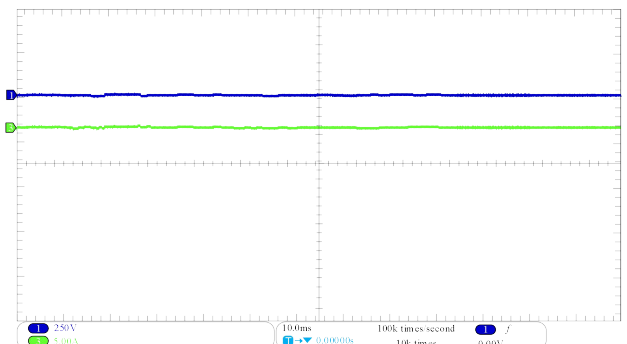
In the above Figures, V_o represents the output voltage waveform, and u_s represents the superimposed disturbance AC voltage. In order to highlight the contrast effect, the voltage waveform of u_s is scaled 15 times and translated to 600 V. The simulation waveforms show that the output voltage of the charger converter under the double closed-loop cascade control strategy fluctuates due to the interference of the input disturbance voltage, and the fluctuation amplitude is ± 5 V, accounting for 16% of the disturbance voltage fluctuation amplitude. The output voltage fluctuation amplitude under the modulation wave selection control strategy of the charger converter is also ± 5 V, but it can be recovered by rapid adjustment. It can be concluded from the waveform that the modulation wave selection control strategy has faster voltage regulation speed and stronger anti-power disturbance ability than the traditional double closed-loop cascade control strategy.

V. SEMI-PHYSICAL PLATFORM EXPERIMENTAL VERIFICATION

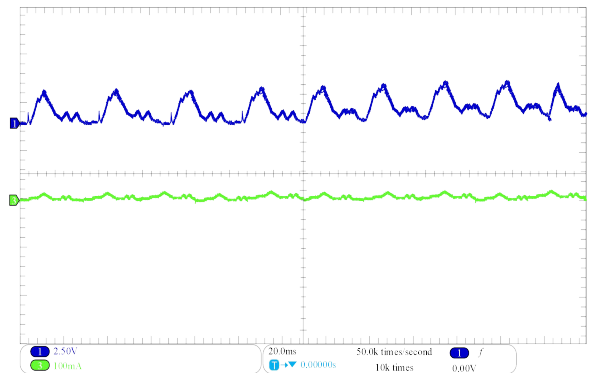
In order to further verify the correctness and feasibility of the proposed circuit and control strategy, this chapter builds a 15 kW charger prototype experimental platform to verify the correctness and feasibility of the circuit and control strategy designed in the previous article, and selects the double closed-loop cascade control strategy as a representative of other algorithm strategies for comparative experiments. The superiority of the modulation wave selection control strategy

is obtained by comparison. The prototype module is shown in Fig.25.

In Fig.25, A module is rectifier, B module is support capacitor, C module is inverter, D module is rectifier bridge, E module is filter, F module is blocking capacitor, G module is switch drive board, H module is isolation transformer, I module is control module. The input voltage of the charging module is 380 V, the maximum output voltage can reach 750 V, and the maximum output current is 25 A. The DC voltage output by the rectifier is used as the input voltage of the subsequent DC / DC converter.



(a) Voltage and current steady-state waveform



(b) Voltage and current ripple

FIGURE 26. Full load feasibility verification waveform.

A. FEASIBILITY VALIDATION

The load is set to 37Ω , the output voltage of the prototype is set to 750 V, and the current limit is 20 A. The modulation wave selection control strategy is used to obtain the output voltage waveform of the charging module under the full load condition of the ZVS half-bridge three-level circuit design, as shown in Fig.26.

As can be seen from Fig.26, the output voltage and current are relatively stable, indicating that the prototype module under the modulation wave selection control strategy can work stably, and the steady-state error is basically zero, and the ripple is only 0.2 %, which well verifies the feasibility of the circuit design and control strategy proposed in this paper.

B. CHARGING POWER SWITCHING EXPERIMENT

When the charging power changes, the charging current will also change. Generally, the voltage level that the battery can withstand is limited, and the charging efficiency can only be improved by increasing the charging current. The prototype module is used to simulate the working condition of the power change of the charger. The output voltage is set to 600 V, and the load is set to 36 Ω. The charging power is divided into fast charging and slow charging, which correspond to the current limit values of 15 A and 10 A, respectively. The experimental output waveform is shown in Fig. 27.

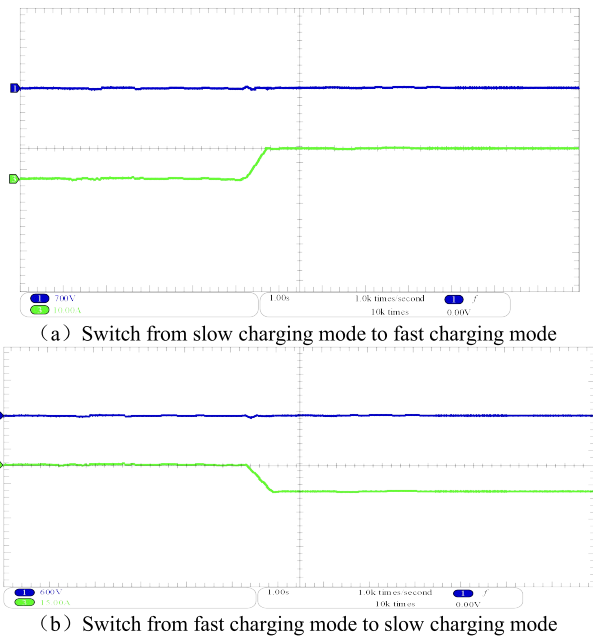


FIGURE 27. Full load feasibility verification waveform.

From the experimental waveforms, it can be seen that when the charging mode is switched, the output voltage is stabilized at the given value of the voltage immediately after only slight fluctuations under the voltage loop control, and the output current rises gently or drops to the current limiting value and remains stable. The charging power changes with the change of the current, and the switching of the charging mode is realized. The experiment further verifies the correctness and feasibility of the designed circuit and control strategy.

C. LOAD MUTATION DISTURBANCE EXPERIMENT

From the previous theoretical research and simulation analysis of the double closed-loop control strategy and the modulation wave selection control strategy, it can be seen that when the load changes, the modulation wave selection control strategy has faster adjustment speed and stronger anti-disturbance ability. The current prototype module designs load change scenarios for more in-depth experimental verification. The output voltage of the experiment is set to 600 V, and the input load is instantaneously reduced from 240 Ω to 120 Ω. The output waveform is as follows.

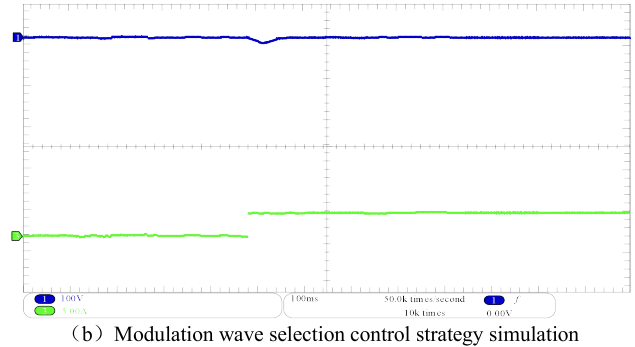
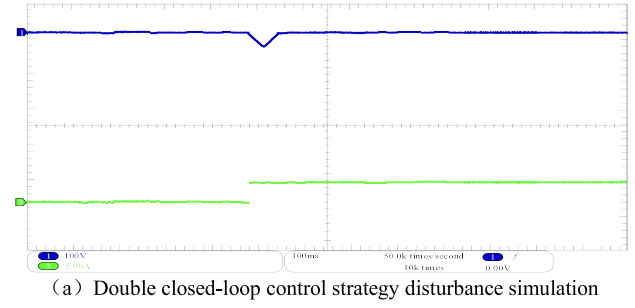


FIGURE 28. Load mutation experiment waveform.

It can be seen from Fig.28 that the output voltage of the prototype module under the two control strategies can be stably maintained at 600 V before the load mutation. When the load mutation occurs, the output voltage of the prototype under the double closed-loop strategy fluctuates greatly and the decrease amplitude reaches 50 V, while the output voltage of the prototype under the modulation wave strategy fluctuates greatly and the decrease amplitude does not exceed 8 V. It can be verified by this group of experiments that the modulation wave strategy can adjust more quickly when the load fluctuates, and its anti-disturbance ability is stronger and the response speed is faster.

VI. CONCLUSION

In this paper, the design principle and operation loss of the traditional charger are analyzed firstly. On this basis, the topology and control strategy of a zero-voltage switching half-bridge DC/DC converter are designed. The conclusions are as follows:

- (1) The modulation wave selection control strategy can realize the constant voltage and current limiting charging control and module parallel current sharing control which are not available in the traditional double closed-loop cascade control strategy. It is very suitable for the multi-module parallel control system of charger.
- (2) Under the same load disturbance, the regulating time of suppressing voltage fluctuation of charger converter under two control strategies has little difference, but the amplitude of output voltage fluctuation under modulation wave selection control strategy is much smaller than that under double closed-loop cascade control strategy.
- (3) The modulation wave selection control strategy has faster voltage regulation speed and stronger anti-power

disturbance ability than the double closed-loop cascade control strategy, and the dynamic performance is better than the latter.

REFERENCES

- [1] L. Tan, N. Zhu, and B. Wu, "An integrated inductor for eliminating circulating current of parallel three-level DC–DC converter-based EV fast charger," *IEEE Trans. Ind. Electron.*, vol. 63, no. 3, pp. 1362–1371, Mar. 2016, doi: [10.1109/TIE.2015.2496904](https://doi.org/10.1109/TIE.2015.2496904).
- [2] I.-O. Lee, "Hybrid DC–DC converter with phase-shift or frequency modulation for NEV battery charger," *IEEE Trans. Ind. Electron.*, vol. 63, no. 2, pp. 884–893, Feb. 2016, doi: [10.1109/TIE.2015.2477345](https://doi.org/10.1109/TIE.2015.2477345).
- [3] S. A. Huang, C.-M. Liaw, and J.-Y. Ni, "Interleaving DC/DC converter-fed electric skateboard with power factor corrected charger," in *Proc. 41st Annu. Conf. IEEE Ind. Electron. Soc.*, Yokohama, Japan, Nov. 2015, pp. 003792–003797, doi: [10.1109/IECON.2015.7392691](https://doi.org/10.1109/IECON.2015.7392691).
- [4] M. R. Sindhu, "A PFC based onboard battery charger using isolated full-bridge DC–DC converter for electric vehicle application," in *Proc. IEEE IAS Global Conf. Emerg. Technol. (GlobConET)*, Arad, Romania, May 2022, pp. 581–586, doi: [10.1109/GlobConET53749.2022.9872512](https://doi.org/10.1109/GlobConET53749.2022.9872512).
- [5] I. Febriyandi, F. D. Wijaya, and E. Firmansyah, "DC–DC converter as power supply of battery charger 100 V 300 W using 25 kHz switching frequency," in *Proc. Int. Conf. Electr. Eng. Comput. Sci. (ICEECS)*, Kuta, Bali, Indonesia, Nov. 2014, pp. 302–307, doi: [10.1109/ICEECS.2014.7045267](https://doi.org/10.1109/ICEECS.2014.7045267).
- [6] Y.-C. Chuang and Y.-L. Ke, "High-efficiency and low-stress ZVT–PWM DC-to-DC converter for battery charger," *IEEE Trans. Ind. Electron.*, vol. 55, no. 8, pp. 3030–3037, Aug. 2008, doi: [10.1109/TIE.2008.921218](https://doi.org/10.1109/TIE.2008.921218).
- [7] B.-K. Lee, J.-P. Kim, S.-G. Kim, and J.-Y. Lee, "A PWM SRT DC/DC converter for 6.6-kW EV onboard charger," *IEEE Trans. Ind. Electron.*, vol. 63, no. 2, pp. 894–902, Feb. 2016, doi: [10.1109/TIE.2015.2480384](https://doi.org/10.1109/TIE.2015.2480384).
- [8] L. Tan, B. Wu, S. Rivera, and V. Yaramasu, "Comprehensive DC power balance management in high-power three-level DC–DC converter for electric vehicle fast charging," *IEEE Trans. Power Electron.*, vol. 31, no. 1, pp. 89–100, Jan. 2016, doi: [10.1109/TPEL.2015.2397453](https://doi.org/10.1109/TPEL.2015.2397453).
- [9] H. Heydari-Doostabad, S. H. Hosseini, R. Ghazi, and T. O'Donnell, "Pseudo DC-link EV home charger with a high semiconductor device utilization factor," *IEEE Trans. Ind. Electron.*, vol. 69, no. 3, pp. 2459–2469, Mar. 2022, doi: [10.1109/TIE.2021.3065623](https://doi.org/10.1109/TIE.2021.3065623).
- [10] Y.-S. Lee and B.-T. Lin, "Adding active clamping and soft switching to boost-flyback single-stage isolated power-factor-corrected power supplies," *IEEE Trans. Power Electron.*, vol. 12, no. 6, pp. 1017–1027, Nov. 1997, doi: [10.1109/63.641500](https://doi.org/10.1109/63.641500).
- [11] H.-L. Jou, K.-D. Wu, Y.-H. Shen, W.-F. Liao, and J.-C. Wu, "Novel isolated asymmetrical T-type DC–DC battery charger," in *Proc. 13th IEEE Conf. Ind. Electron. Appl. (ICIEA)*, Wuhan, China, May 2018, pp. 1352–1356, doi: [10.1109/ICIEA.2018.8397919](https://doi.org/10.1109/ICIEA.2018.8397919).
- [12] L. Luo, "A novel hybrid resonant PI controller to decrease DC capacitance for EV charger," in *Proc. IEEE Conf. Expo Transp. Electrific. Asia-Pacific (ITEC Asia-Pacific)*, Beijing, China, Aug. 2014, pp. 1–3, doi: [10.1109/ITEC-AP.2014.6940795](https://doi.org/10.1109/ITEC-AP.2014.6940795).
- [13] C. F. Oliveira, J. L. Afonso, and V. Monteiro, "A bidirectional multilevel DC–DC converter applied to a bipolar DC grid: Analysis of operation under fault conditions," in *Proc. Int. Young Eng. Forum (YEF-ECE)*, Caparica/Lisboa, Portugal, Jul. 2021, pp. 38–43, doi: [10.1109/YEF-ECE52297.2021.9505140](https://doi.org/10.1109/YEF-ECE52297.2021.9505140).
- [14] Y. Jang, D. L. Dillman, and M. M. Jovanovic, "A new soft-switched PFC boost rectifier with integrated flyback converter for stand-by power," *IEEE Trans. Power Electron.*, vol. 21, no. 1, pp. 66–72, Jan. 2006, doi: [10.1109/TPEL.2005.861123](https://doi.org/10.1109/TPEL.2005.861123).
- [15] B. Fitzgerald, "A new family of zero voltage switching power supplies," *IEEE Trans. Consum. Electron.*, vol. 43, no. 3, pp. 961–964, Aug. 1997, doi: [10.1109/30.628773](https://doi.org/10.1109/30.628773).
- [16] L. Xue, Z. Shen, D. Boroyevich, P. Mattavelli, and D. Diaz, "Dual active bridge-based battery charger for plug-in hybrid electric vehicle with charging current containing low frequency ripple," *IEEE Trans. Power Electron.*, vol. 30, no. 12, pp. 7299–7307, Dec. 2015, doi: [10.1109/TPEL.2015.2413815](https://doi.org/10.1109/TPEL.2015.2413815).
- [17] F. Musavi, M. Craciun, D. S. Gautam, and W. Eberle, "Control strategies for wide output voltage range LLC resonant DC–DC converters in battery chargers," *IEEE Trans. Veh. Technol.*, vol. 63, no. 3, pp. 1117–1125, Mar. 2014, doi: [10.1109/TVT.2013.2283158](https://doi.org/10.1109/TVT.2013.2283158).
- [18] L. Tan, B. Wu, V. Yaramasu, S. Rivera, and X. Guo, "Effective voltage balance control for bipolar-DC-bus-fed EV charging station with three-level DC–DC fast charger," *IEEE Trans. Ind. Electron.*, vol. 63, no. 7, pp. 4031–4041, Jul. 2016, doi: [10.1109/TIE.2016.2539248](https://doi.org/10.1109/TIE.2016.2539248).
- [19] M. Antivachis, J. A. Anderson, D. Bortis, and J. W. Kolar, "Analysis of a synergetically controlled two-stage three-phase DC/AC buck-boost converter," *CPSS Trans. Power Electron. Appl.*, vol. 5, no. 1, pp. 34–53, Mar. 2020, doi: [10.24295/CPSSSTPEA.2020.00004](https://doi.org/10.24295/CPSSSTPEA.2020.00004).
- [20] W.-S. Lee, J.-H. Kim, J.-Y. Lee, and I.-O. Lee, "Design of an isolated DC/DC topology with high efficiency of over 97% for EV fast chargers," *IEEE Trans. Veh. Technol.*, vol. 68, no. 12, pp. 11725–11737, Dec. 2019, doi: [10.1109/TVT.2019.2949080](https://doi.org/10.1109/TVT.2019.2949080).
- [21] B. Gu, J.-S. Lai, N. Kees, and C. Zheng, "Hybrid-switching full-bridge DC–DC converter with minimal voltage stress of bridge rectifier, reduced circulating losses, and filter requirement for electric vehicle battery chargers," *IEEE Trans. Power Electron.*, vol. 28, no. 3, pp. 1132–1144, Mar. 2013, doi: [10.1109/TPEL.2012.2210565](https://doi.org/10.1109/TPEL.2012.2210565).
- [22] Y.-J. Lee, A. Khaligh, and A. Emadi, "Advanced integrated bidirectional AC/DC and DC/DC converter for plug-in hybrid electric vehicles," *IEEE Trans. Veh. Technol.*, vol. 58, no. 8, pp. 3970–3980, Oct. 2009, doi: [10.1109/TVT.2009.2028070](https://doi.org/10.1109/TVT.2009.2028070).
- [23] H. Karneddi and D. Ronanki, "Universal bridgeless nonisolated battery charger with wide-output voltage range," *IEEE Trans. Power Electron.*, vol. 38, no. 3, pp. 2816–2820, Mar. 2023, doi: [10.1109/TPEL.2022.3217943](https://doi.org/10.1109/TPEL.2022.3217943).
- [24] V. M. Iyer, S. Guler, and S. Bhattacharya, "Small-signal stability assessment and active stabilization of a bidirectional battery charger," *IEEE Trans. Ind. Appl.*, vol. 55, no. 1, pp. 563–574, Jan. 2019, doi: [10.1109/TIA.2018.2871101](https://doi.org/10.1109/TIA.2018.2871101).
- [25] V. Monteiro, J. C. Ferreira, A. A. N. Meléndez, C. Couto, and J. L. Afonso, "Experimental validation of a novel architecture based on a dual-stage converter for off-board fast battery chargers of electric vehicles," *IEEE Trans. Veh. Technol.*, vol. 67, no. 2, pp. 1000–1011, Feb. 2018, doi: [10.1109/TVT.2017.2755545](https://doi.org/10.1109/TVT.2017.2755545).
- [26] V. R. K. Kanamarlapudi, B. Wang, N. K. Kandasamy, and P. L. So, "A new ZVS full-bridge DC–DC converter for battery charging with reduced losses over full-load range," *IEEE Trans. Ind. Appl.*, vol. 54, no. 1, pp. 571–579, Jan. 2018, doi: [10.1109/TIA.2017.2756031](https://doi.org/10.1109/TIA.2017.2756031).
- [27] M. A. Alharbi, A. M. Alcaide, M. Dahidah, S. Ethni, V. Pickert, and J. I. Leon, "Rotating phase shedding for interleaved DC–DC converter-based EVs fast DC chargers," *IEEE Trans. Power Electron.*, vol. 38, no. 2, pp. 1901–1909, Feb. 2023, doi: [10.1109/TPEL.2022.3211864](https://doi.org/10.1109/TPEL.2022.3211864).
- [28] R. Ren, B. Liu, E. A. Jones, F. F. Wang, Z. Zhang, and D. Costinett, "Capacitor-clamped, three-level GaN-based DC–DC converter with dual voltage outputs for battery charger applications," *IEEE J. Emerg. Sel. Topics Power Electron.*, vol. 4, no. 3, pp. 841–853, Sep. 2016, doi: [10.1109/JESTPE.2016.2586890](https://doi.org/10.1109/JESTPE.2016.2586890).
- [29] R. Soares, N. Djekanovic, O. Wallmark, and P. C. Loh, "Integration of magnified alternating current in battery fast chargers based on DC–DC converters using transformerless resonant filter design," *IEEE Trans. Transport. Electrific.*, vol. 5, no. 4, pp. 925–933, Dec. 2019, doi: [10.1109/TTE.2019.2920328](https://doi.org/10.1109/TTE.2019.2920328).
- [30] W.-Y. Choi, M.-K. Yang, and H.-S. Cho, "High-frequency-link soft-switching PWM DC–DC converter for EV on-board battery chargers," *IEEE Trans. Power Electron.*, vol. 29, no. 8, pp. 4136–4145, Aug. 2014, doi: [10.1109/TPEL.2013.2288364](https://doi.org/10.1109/TPEL.2013.2288364).
- [31] J. Linru, Z. Yuanxing, L. Taoyong, D. Xiaohong, and Z. Jing, "Analysis on charging safety and optimization of electric vehicles," in *Proc. IEEE 6th Int. Conf. Comput. Commun. (ICCC)*, Chengdu, China, Dec. 2020, pp. 2382–2385, doi: [10.1109/ICCC51575.2020.9344906](https://doi.org/10.1109/ICCC51575.2020.9344906).
- [32] Z. Ye, Y. Gao, and N. Yu, "Learning to operate an electric vehicle charging station considering vehicle-grid integration," *IEEE Trans. Smart Grid*, vol. 13, no. 4, pp. 3038–3048, Jul. 2022, doi: [10.1109/TSG.2022.3165479](https://doi.org/10.1109/TSG.2022.3165479).
- [33] K. Schwenk, S. Meisenbacher, B. Briegel, T. Harr, V. Hagenmeyer, and R. Mikut, "Integrating battery aging in the optimization for bidirectional charging of electric vehicles," *IEEE Trans. Smart Grid*, vol. 12, no. 6, pp. 5135–5145, Nov. 2021, doi: [10.1109/TSG.2021.3099206](https://doi.org/10.1109/TSG.2021.3099206).
- [34] B. Al-Hanahi, I. Ahmad, D. Habibi, and M. A. S. Masoum, "Charging infrastructure for commercial electric vehicles: Challenges and future works," *IEEE Access*, vol. 9, pp. 121476–121492, 2021, doi: [10.1109/ACCESS.2021.3108817](https://doi.org/10.1109/ACCESS.2021.3108817).

- [35] Z. J. Lee, S. Sharma, D. Johansson, and S. H. Low, "ACN-sim: An open-source simulator for data-driven electric vehicle charging research," *IEEE Trans. Smart Grid*, vol. 12, no. 6, pp. 5113–5123, Nov. 2021, doi: [10.1109/TSG.2021.3103156](https://doi.org/10.1109/TSG.2021.3103156).
- [36] J.-H. Ahn and B. K. Lee, "High-efficiency adaptive-current charging strategy for electric vehicles considering variation of internal resistance of lithium-ion battery," *IEEE Trans. Power Electron.*, vol. 34, no. 4, pp. 3041–3052, Apr. 2019, doi: [10.1109/TPEL.2018.2848550](https://doi.org/10.1109/TPEL.2018.2848550).
- [37] A. Radic, A. Straka, and A. Prodic, "Synchronized zero-crossing-based self-tuning capacitor time-constant estimator for low-power digitally controlled DC–DC converters," *IEEE Trans. Power Electron.*, vol. 29, no. 10, pp. 5106–5110, Oct. 2014, doi: [10.1109/TPEL.2014.2313727](https://doi.org/10.1109/TPEL.2014.2313727).
- [38] M. Brunoro and J. L. F. Vieira, "A high-performance ZVS full-bridge DC–DC 0–50-V/0–10-A power supply with phase-shift control," *IEEE Trans. Power Electron.*, vol. 14, no. 3, pp. 495–505, May 1999, doi: [10.1109/63.761693](https://doi.org/10.1109/63.761693).
- [39] S.-Y. Ou and H.-P. Hsiao, "Analysis and design of a novel single-stage switching power supply with half-bridge topology," *IEEE Trans. Power Electron.*, vol. 26, no. 11, pp. 3230–3241, Nov. 2011, doi: [10.1109/TPEL.2011.2141688](https://doi.org/10.1109/TPEL.2011.2141688).
- [40] M. R. A. Siddique, M. J. Ferdous, and I. Islam, "Charge pump capacitor based high voltage gain DC–DC step-up converter," in *Proc. Int. Conf. Inform., Electron. Vis. (ICIEV)*, Dhaka, Bangladesh, May 2014, pp. 1–4, doi: [10.1109/ICIEV.2014.6850704](https://doi.org/10.1109/ICIEV.2014.6850704).
- [41] S. H. Hosseini, R. Ghazi, and H. Heydari-Doostabad, "An extendable quadratic bidirectional DC–DC converter for V2G and G2V applications," *IEEE Trans. Ind. Electron.*, vol. 68, no. 6, pp. 4859–4869, Jun. 2021, doi: [10.1109/TIE.2020.2992967](https://doi.org/10.1109/TIE.2020.2992967).
- [42] M. A. H. Rafi and J. Bauman, "Optimal control of semi-dual active bridge DC/DC converter with wide voltage gain in a fast-charging station with battery energy storage," *IEEE Trans. Transport. Electrification*, vol. 8, no. 3, pp. 3164–3176, Sep. 2022, doi: [10.1109/TTE.2022.3170737](https://doi.org/10.1109/TTE.2022.3170737).
- [43] H. Obara, M. Katayama, A. Kawamura, J. Xu, and N. Shimosato, "A modular multilevel DC–DC converter with auxiliary inductor circuits for cell voltage balancing and fast output response," *IEEE Open J. Power Electron.*, vol. 3, pp. 391–401, 2022, doi: [10.1109/OJPEL.2022.3185645](https://doi.org/10.1109/OJPEL.2022.3185645).
- [44] J. D. Boles, J. J. Piel, and D. J. Perreault, "Enumeration and analysis of DC–DC converter implementations based on piezoelectric resonators," *IEEE Trans. Power Electron.*, vol. 36, no. 1, pp. 129–145, Jan. 2021, doi: [10.1109/TPEL.2020.3004147](https://doi.org/10.1109/TPEL.2020.3004147).
- [45] S. Nakata, H. Makino, J. Hosokawa, T. Yoshimura, S. Iwade, and Y. Matsuda, "Energy efficient stepwise charging of a capacitor using a DC–DC converter with consecutive changes of its duty ratio," *IEEE Trans. Circuits Syst. I, Reg. Papers*, vol. 61, no. 7, pp. 2194–2203, Jul. 2014, doi: [10.1109/TCSL.2013.2295895](https://doi.org/10.1109/TCSL.2013.2295895).
- [46] J. Zeng, X. Du, and Z. Yang, "A multiport bidirectional DC–DC converter for hybrid renewable energy system integration," *IEEE Trans. Power Electron.*, vol. 36, no. 11, pp. 12281–12291, Nov. 2021, doi: [10.1109/TPEL.2021.3082427](https://doi.org/10.1109/TPEL.2021.3082427).
- [47] B. Arntzen and D. Maksimovic, "Switched-capacitor DC/DC converters with resonant gate drive," *IEEE Trans. Power Electron.*, vol. 13, no. 5, pp. 892–902, Sep. 1998, doi: [10.1109/63.712304](https://doi.org/10.1109/63.712304).



RONG YAN received the B.S. degree in aviation and aerospace from Shanghai Jiao Tong University, Shanghai, China, in 2012, and the M.S. degree in power machinery and engineering from Tongji University, Shanghai, in 2015. From 2015 to 2018, he was a Powertrain Engineer with the Technical Center, SAIC Motor Corporation Ltd. Since 2019, he has been the Admin Manager of the Chief Engineer Office and the Director of smart energy with Shanghai Aowei Technology Development

Company Ltd. He holds ten granted patents and software copyrights. His current research interests include the integration and thermal management of power batteries, portable vehicle fast charging systems, the application of supercapacitors in smart energy, and harmonic treatment. He is a member of the Chinese Society for Internal Combustion Engines and the Shanghai Transportation Trade Association.



JUNNAN ZHOU received the degree from the Beijing University of Science and Technology. He is currently the Deputy Director of the Party Building Department (Propaganda Department), State Grid Shanghai Power Supply Company, where he is mainly responsible for the company's news publicity, brand building, public opinion control, and social responsibility. He has published in the field of industry, power equipment, and other journals: problems and solutions in the

transformation of power marketing measurement, the fine management analysis of power marketing industry expansion process, and how to apply power marketing inspection to improve power marketing efficiency.



LIN PAN received the degree from the Shanghai University of Electric Power, in August 2002. In 2002, he joined the Shanghai Electric Power Company, where he was responsible for relay protection. While doing a good job in daily work, he actively participated in the compilation of various articles and professional books and wrote many articles, such as "Analysis of relay protection problems and measures in substation operation," "Analysis of daily maintenance and

maintenance methods of power operation equipment," and "Analysis of technical management of power operation and maintenance," which were published in journals. The "Induction training manual for distribution network system employees (substation section)" has also been officially published.



DONGJUNMING YANG received the bachelor's degree in electrical engineering and automation from North China Electric Power University, in 2019, and the master's degree in electrical engineering from North China Electric Power University, in 2022. In 2022, he joined the Power Grid Planning Research Center, Guizhou Power Grid Company Ltd., where he held the position of one-time evaluation of substation. He has published one SCI search article, five EI search articles,

three invention patents, and two soft works. His current research interests include new energy power generation and grid connection, distributed energy storage, and retired power battery cascade utilization.

...



HAODONG SHEN was born in 1985. He is currently the Deputy Director of the Technology Research and Development Center, East China Electric Power Test and Research Institute Company Ltd.; and a Senior Engineer, a Chief Technician of Shanghai, a Shanghai Technician, and a Provincial Excellent Expert with the State Grid Corporation of China. He has served as the State Grid Shanghai Electric Power Company Control Center Power Grid Application Director of State Grid Shanghai Energy Internet Research Institute Company Ltd., and an Intelligent Distribution and Utilization Technology Center Deputy Director. He has engaged in power dispatching and scientific and technological innovation, with rich scientific and technological research and development and engineering demonstration experience.